Available online at www.sciencedirect.com
SCIENCE DIRECT
Thermochimica Acta 445 (2006) 144–150
thermochimica acta
www.elsevier.com/locate/tca

A new micro-fluid chip calorimeter for biochemical applications

J. Lerchner [a,*], A. Wolf [a], G. Wolf [a], V. Baier [b], E. Kessler [b], M. Nietzsch [c], M. Krügel [c]

[a] *TU Bergakademie Freiberg, Institute of Physical Chemistry, Leipziger Str. 29, D-09596 Freiberg, Germany*
[b] *Institute of Physical High Technology, Albert-Einstein-Str. 9, D-07742 Jena, Germany*
[c] *"Eurotronics" Gesellschaft f. wiss. Gerätebau mbH, Leipzig, Weissenfelser Strasse 67, D-04229 Leipzig, Germany*

Available online 2 September 2005

Abstract

Based on a new thermopile heat power sensor, which was developed in MEMS technology, a miniaturized flow-through calorimeter was constructed. The heat power sensor consists of a silicon chip with a thin film BiSb/Sb thermopile and a PMMA reaction chamber. To ensure high signal resolution the heat power sensor is mounted inside a high-precision thermostat, which has a temperature stability of less than 100 μK. The heat power sensitivity of the calorimeter is 4–7 V W^{-1} depending on the thermal conductivity of the liquid, the height of the chosen reaction chamber and the volume flow rate. A limit of detection of less than 50 nW can be obtained for volume flows lower than 5 μl min^{-1}. An important advantage is the low sample consumption of the calorimeter. For special applications the sample need for one measurement pulse does not exceed 20 μl.

Keywords: Chip calorimetry; Thin-film thermopiles; Enzyme screening; Microbial heat power detection

1. Introduction

Calorimetry is a powerful tool for analyzing biochemical processes, e.g. enzyme catalyzed reactions and metabolic activities of microorganisms or living cells [1]. Because heat production is not reaction specific calorimetry is applicable to a wide range of reactions and does not require any labeling or immobilization of the reactants. The invention of miniaturized, silicon chip based calorimeters opened new opportunities. One of the advantages of silicon chip based calorimeters is their capability of analyzing small sample quantities and the fast operation due to the small time constants. This favors them for screening applications especially if high-cost materials are investigated. For example, a micro-machined calorimetric biosensor with integrated micro-fluidic channels and a 15 nl reaction chamber was presented by Zhang and Tadigadapa [2]. Johannessen et al. [3] designed a calorimeter with a sample chamber of 0.72 nl for measuring the metabolism of single living cells. Chip calorimeter arrays presented by Torres et al. [4] and Vivactis [5] need sample volumes of less than 1 μl and are useful for high throughput investigations of biochemical materials.

The suitability of ultra low sample volume calorimeters for bioprocess control suffers from their low volume-specific sensitivity. Usually the heat capacity of the addenda of silicon chip based calorimeters is in the range of μJ K^{-1}. If the time constant of the studied process does not exceed several seconds the limit of detection is essentially determined by the resolution of the temperature measurement and less influenced by the volume of the sample, i.e. a reasonable application of nanoliter calorimeters (Torres, Vivactis) is restricted to fast reactions. If slow processes are studied, e.g. metabolic heat production of microorganism or slow enzyme catalyzed reactions, the magnitude of the signal is dependent on the sample volume and the volume specific detection limit increases in turn with the miniaturization. For example, the detection limit of the Johannessen calorimeter is 18 W l^{-1}, whereas those of the well know TAM2277 calorimeter is 50 μW l^{-1}. In order to monitor the metabolic heat production of bacteria, a volume specific detection limit of approximately 0.2 mW l^{-1} is necessary, if cell densities lower than 10^5 ml^{-1} are to be detected (10 pW $cell^{-1}$ assumed). Consequently, miniaturized calorimeters are to be optimized regard-

* Corresponding author. Tel.: +49 3731 393588; fax: +49 3731 392125.
E-mail address: johannes.larchner@chemie.tu-freiberg.de (J. Lerchner).

0040-6031/$ – see front matter © 2005 Elsevier B.V. All rights reserved.
doi:10.1016/j.tca.2005.07.011

ing chamber volume and sensitivity. To assure fast response and reasonable sample consumption the chamber volume should not exceed several micro-liters. On the other hand, a volume specific heat power resolution of only a few $mW\,l^{-1}$ is desirable for relevant applications, which requires absolute heat power resolutions less than 100 nW.

With the described calorimeter we aim to demonstrate a device which meets to a considerable degree the abovementioned requirements: the needed sample volume of 10–20 μl permits the application of rare biochemical substances. The fast response enables the calorimeter as process control device. A nano-watt detection limit offers a wide range of biochemical applications. The design of the presented calorimeter is based on experiences obtained from former versions of miniaturized flow-through calorimeters developed in our laboratory [6,7].

2. Experimental

2.1. Thin-film thermopile module as heat power transducer

Fig. 1 shows the top view of the thermopile calorimeter chip MFK 472 which was applied as heat power transducer. It is a strongly improved version of thermopile devices which were developed in the IPHT in recent years [8]. The thermopile chip is based on SU-8 technology and consists of four distinct thermopile areas and heating elements underneath, which correspond to four electronic measuring sections, glue bonded onto a copper heat sink and wire bonded to a PCB carrier. Each of the thermopiles consists of 118 BiSb/Sb thin-film thermocouples deposited on a 1 μm silicon nitride membrane. The thin-film heaters are made of NiCr. The conversion of a defined electrical heating power delivers a roughly measure of the sensitivity of each thermopile by relating the output voltage of a given thermopile to the electrical power converted in the corresponding heater. The four thermopiles which are subsequently arranged in the flow direction allow

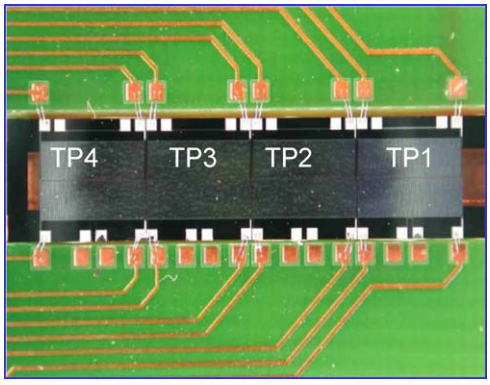

Fig. 1. Top view of the calorimetric chip MFK 472 (IPHT) with four independent readable thermopile segments.

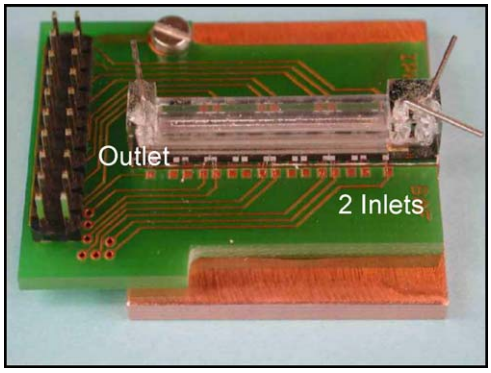

Fig. 2. Calorimetric chip module with PMMA reaction chamber and copper plate heat sink.

to resolve the transient behavior of a reaction which is starting immediately after the mixing of the reactants. A photograph of the complete calorimetric chip module is depicted in Fig. 2. The flow channel has an effective length of 20 mm (inlet to outlet) and a width of 1 mm, respectively. Different heights of the channel are ranging from 0.5 to 1.2 mm. A typical height of 0.5 mm corresponds with a volume of 10 μl in the membrane region. The flow channel consists of PMMA and is micro-machined with a CAM engine. This channel is mounted by epoxy glue onto the silicon chip after wire-bonding to the PCB carrier.

Further details of the manufacturing of the thermopile chip are given in ref. [9].

2.2. The chip-calorimetric system

Based on the developed thermopile heat power transducer a miniaturized flow-through calorimetric system was constructed. The structure of the system is schematically drawn in Fig. 3. To ensure high signal resolution the calorimetric module is mounted inside a high-precision thermostat (Fig. 4), which has a temperature stability of better than 100 μK. The developed two-stage thermostat consists of two nested U-shaped frames. At the outer sides of the walls foil heaters are attached. To enable fast response the control temperature sensors (thermistors 10 kΩ, BetaTherm) are placed inside the walls near the centre of the foil heaters. For temperature control two independent digital PID controllers with optimized parameters are used. The control temperatures for the outer and inner frame are set to 25 and 25.3 °C, respectively. A thermistor temperature sensor is placed inside the copper heat sink of the calorimetric module. The temperature is measured with a resolution of 6 μK and can be utilized for the correction of external temperature perturbations which are not completely suppressed by the thermostat. The inlets of the PMMA reaction chamber are connected with miniaturized piston pumps via Teflon tubes. The piston pumps (LEE LPV50) are part of fluid units and are operated together with sets of micro-valves (LEE LFVA) for reactant selection. Typical volume flow rates are ranged from 5 to 30 $\mu l\,min^{-1}$. Vol-

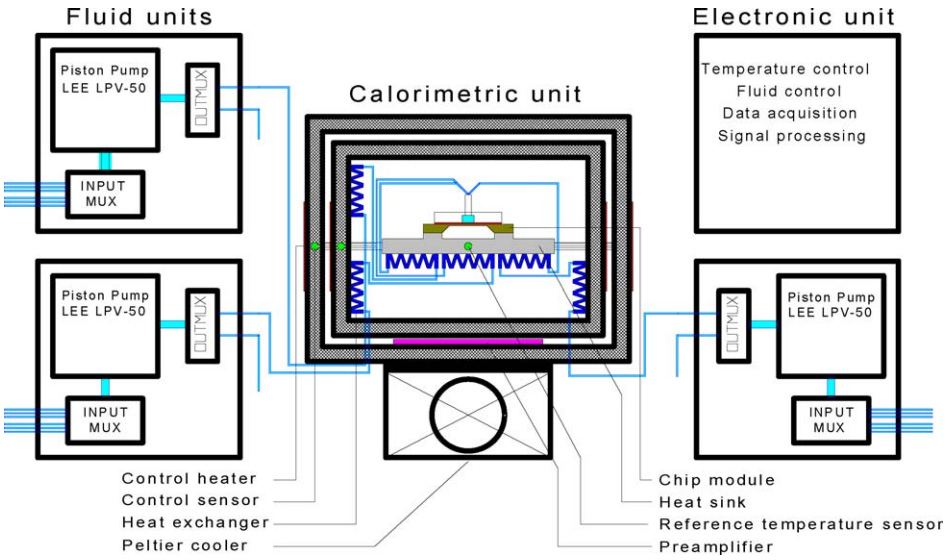

Fig. 3. Scheme of the calorimetric system.

ume flow rates higher than 50 μl min^{-1} exceed the capacity of the fluid heat exchanger. For the temperature equilibration of the liquids micro-machined heat exchangers (IPHT Jena) are used whose dead volumes are 15 μl in each case. At first the liquid flows pass heat exchangers attached at the inner frame of the thermostat. A final temperature equilibration is achieved by heat exchangers attached at the bottom side of the copper heat sink plate. If volume increments of less than 15 μl are injected optimal thermal adaptation of the reactants is assured.

Further, the calorimetric system is equipped with an electronic unit for data acquisition, automatically operation of the fluid units and performing of the temperature control. The user interface is realized by a PC which is connected to the electronic unit.

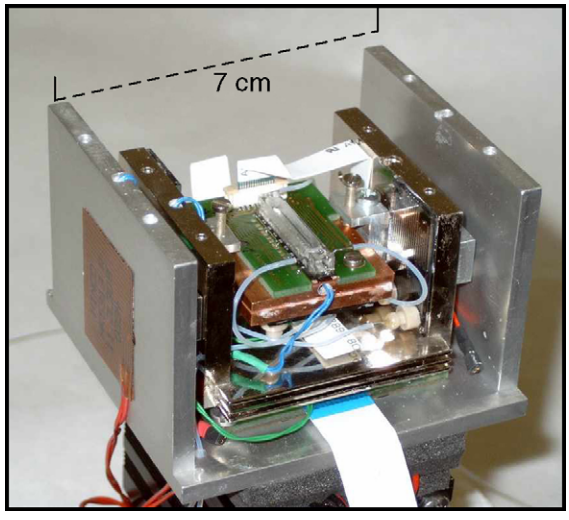

Fig. 4. Calorimetric unit with chip module and thermostat (without lids).

2.3. Modes of operation

Two modes of operation are convenient. In the *continuous injection* mode the reactants are permanently injected with a constant and precisely known volume flow rate to obtain a steady-state output signal. One has to take into account a flow rate dependent sensitivity and a reduced degree of conversion if no appropriate flow rates are applied. In the *impulse injection* mode volume increments which are smaller than the chamber volume are injected. This kind of operation provides voltage peaks from which the peak area has to be calculated. A complete conversion is assured and the sample consumption is minimized. Furthermore, the temperature equilibration of the reactant solutions before injection is improved. On the other hand dead volumes caused by the valves and due to backward diffusion have to be determined.

2.4. Test reactions

To demonstrate the performance of the calorimetric system the results from three enzyme catalyzed reactions are presented: the oxidation of glucose catalyzed by glucose oxidase and catalase, the hydrolysis of penicillin G catalyzed by β-lactamase and the oxidation of ascorbic acid catalyzed by ascorbate oxidase. The reactions were chosen because of their very different K_m values (K_m = 0.2–1.0 mmol l^{-1} and K_m = 30–40 mmol l^{-1} for the oxidation of ascorbic acid and glucose, respectively) and a possibly analytical interest.

The experiments were performed in impulse injection mode with volume increments of 7.5 or 10 μl and using a 16 μl reaction chamber (0.8 mm chamber height). The substrate and enzyme solution increments were simultaneously injected through fluid units 1 and 2, respectively, with 10 μl min^{-1} volume flow rate.

The following enzymes were used: glucose oxidase (EC 1.1.3.4) (SERVA), 250 U ml^{-1}, and catalase (EC 1.11.1.6) (Serva), 270 U ml^{-1}, both from *Aspergillus niger*, β-lactamase (EC 3.5.2.6) (SERVA), 15 U ml^{-1}, from *Bacillus cereus* and ascorbate oxidase (EC 1.10.3.3) (SIGMA), 125 U ml^{-1}, from *cucurbita* sp. The solutions were prepared with phosphate buffer pH 6.9 0.1 mol l^{-1} (oxidation of glucose and hydrolysis of penicillin) and phosphate buffer pH 5.6 0.1 mol l^{-1} (oxidation of ascorbic acid), respectively. The specified enzyme activities are related to the applied solutions.

The D(+)-glucose (Fluka), penicillin G (MERCK) and ascorbic acid (SIGMA) were of grade *for microbiology*. All other chemicals were of analytical grade.

3. Results and discussion

3.1. Limit of detection

Assuming perfect temperature control the limit of detection for the heat power measurement is determined by the electronic noise of the thermopiles and amplifier. A thermal noise of 23 nV for each thermopile is expected for a thermopile resistance $R = 35\,\text{k}\Omega$, the band width $B = 1$ Hz and $T = 298$ K. The typical noise of the applied operational amplifiers (AD8628) is 24 nV (voltage noise 0.1–1 Hz), which results in a total noise of 33 nV for $B = 1$ Hz. The estimated noise level agrees well with the experimentally determined one applying dummy resistors of 35 kΩ. Then, the noise equivalent power of one segment of the thermopile detector can be estimated to 8.3 nW assuming a sensitivity of 4 V W^{-1}.

Under real experimental conditions external temperature fluctuations are dominating the heat power resolution. Obviously, the reference temperature sensor (see Fig. 3) registers sufficiently well these fluctuations, because a deterministic relationship between temperature and signal fluctuations could be found. In order to determine the parameters of an ARX model [10], which is describing this relationship, stochastic temperature fluctuations were induced and both reference temperature and thermopile signal were measured simultaneously. The system identification toolbox of MATLAB (MathWorks Inc., USA) was applied for the parameter estimation. The magnitude of the expected signal fluctuations which are caused by temperature changes can be calculated by the frequency gain (Fig. 5) obtained from the estimated model. At lower frequencies it depends only on the heat capacity of the reaction chamber including the liquid, whereas at higher values the time constant of the device becomes important. From the derived frequency gain one can conclude that only fast temperature changes induce remarkable signal fluctuations. In Fig. 6 the reference temperature and the four thermopile signals are shown for different situations. In case A temperature changes less than 100 μK during several minutes are measured, which have only minor effect on the thermopile signal. In case B temperature oscilla-

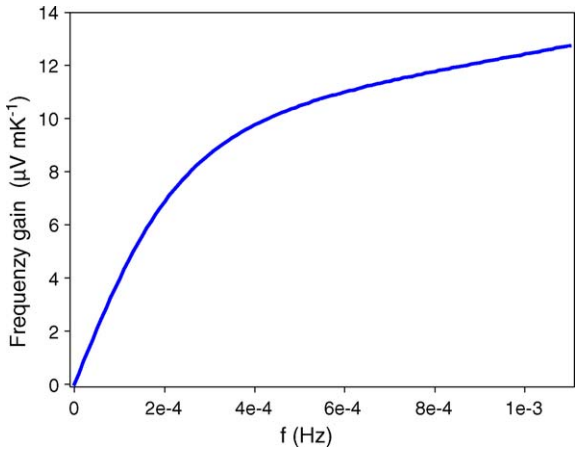

Fig. 5. Experimentally determined frequency gain for the transfer of reference temperature perturbations to the thermopile signals.

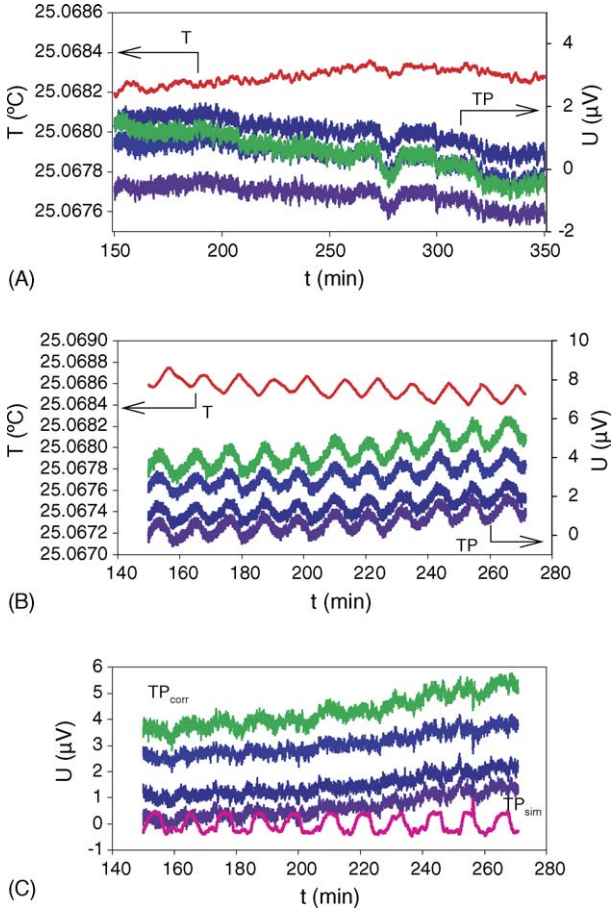

Fig. 6. Correlation between thermopile signals and reference temperature. (A) Low level perturbations. Heat power resolution of 30 nW can be obtained. (B) Correlation between signals and temperature fluctuations in the heat sink. (C) Correction of the distortions applying the temperature-to-signal transfer function. TP$_{sim}$ is the calculated correction signal.

tions of >1 mHz were provoked by manipulation of the room temperature control. In this case remarkable signal deviations with a magnitude of 1 μV arise, which agree with the derived frequency gain. In general, the stability of the reference temperature is better than 100 μK resulting in a heat power detection limit of less than 50 nW.

The estimated model enables the correction of external temperature fluctuations by measuring the reference temperature [11] and simulation of the induced signal deviations. Fig. 6C demonstrates the successful correction of induced signal perturbations using a simulated thermopile signal TP_{sim} which is related to the measured reference temperature.

3.2. Sensitivity and accuracy

Because the reaction chamber is only partially covered by the thermopiles, which is a typical situation for miniaturized, silicon chip based calorimeters [12], the sensitivity of the device depends on the size of the reaction chamber, the heat conductivity of the liquid as well as on the local distribution of the heat power dissipation inside the reaction chamber. Extensive investigations were done in order to characterize the sensitivity of the presented calorimeter by analyzing Joule heating effects using platinum wires located at different positions inside the reaction chamber and by applying appropriate chemical reactions. Detailed results will be published in a separate paper [13]. Here, only a brief summary is given:

- Calorimetric sensitivities 7.2, 6.6, 5.4 $V W^{-1}$ based on TRIS protonization reaction [14] and the hydrolysis of methylparaben [15] are obtained for chamber heights of 0.5, 0.8 and 1.2 mm, respectively.
- The mean sensitivities of the first and the fourth thermopile segment are 8% smaller than that of the other one.
- From the platinum wire based Joule heating measurements sensitivity values were determined, which dependent on the position of the heat power source with respect to the chip membrane. Consequently, the sensitivity gradients induce systematic errors in the case of non-uniform heat power dissipation.
- A first order time constant of 12 s is estimated from Joule heating experiments using an auxiliary platinum wire located in the centre of a 1.2 mm reaction chamber.

3.3. Examples of application

Up to now the device was widely used for the investigation of biochemical reactions. In order to study the microbial growth on-line measurements of the metabolic heat production were performed by periodic injection of bacterial sus-

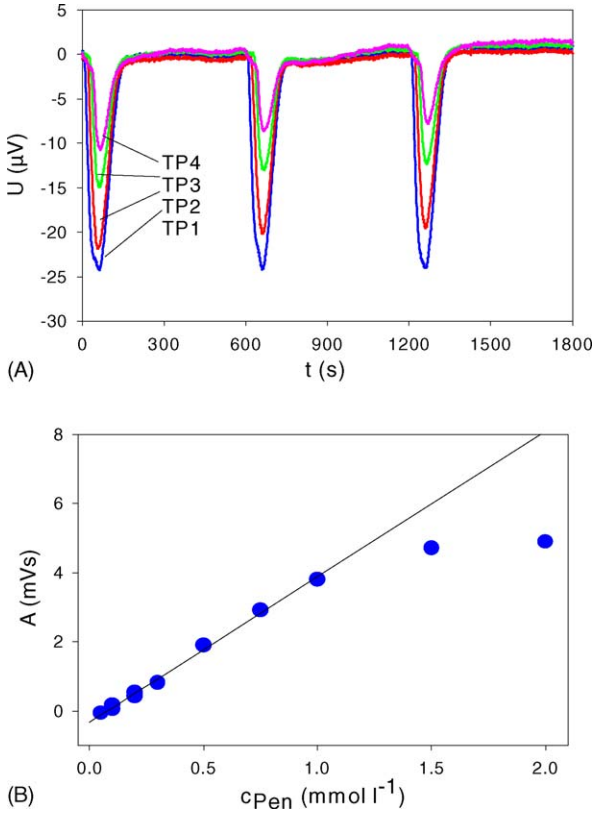

Fig. 7. Hydrolysis of penicillin G by β-lactamase (A: $c = 0.5$ mmol l^{-1}).

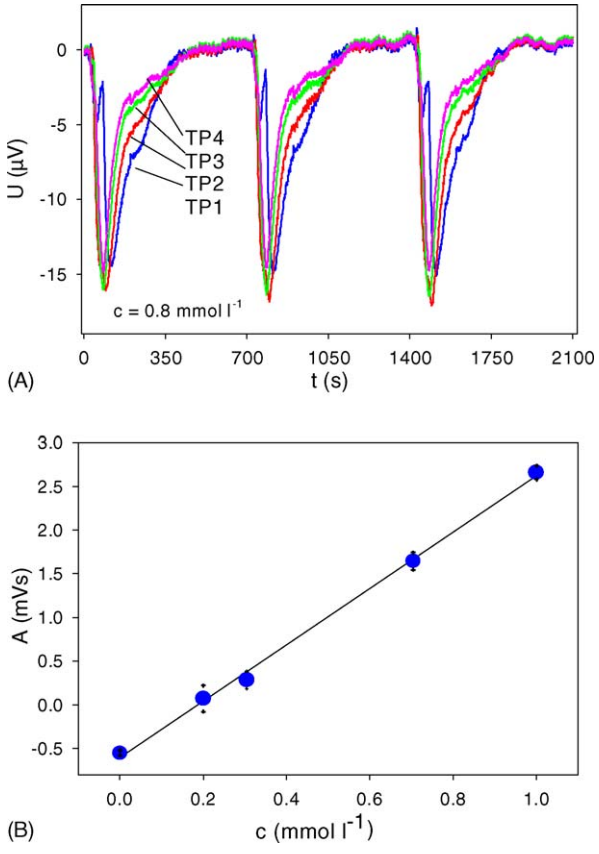

Fig. 8. Oxidation of glucose by glucose oxidase/catalase. (A: $c = 1.0$ mmol l^{-1}).

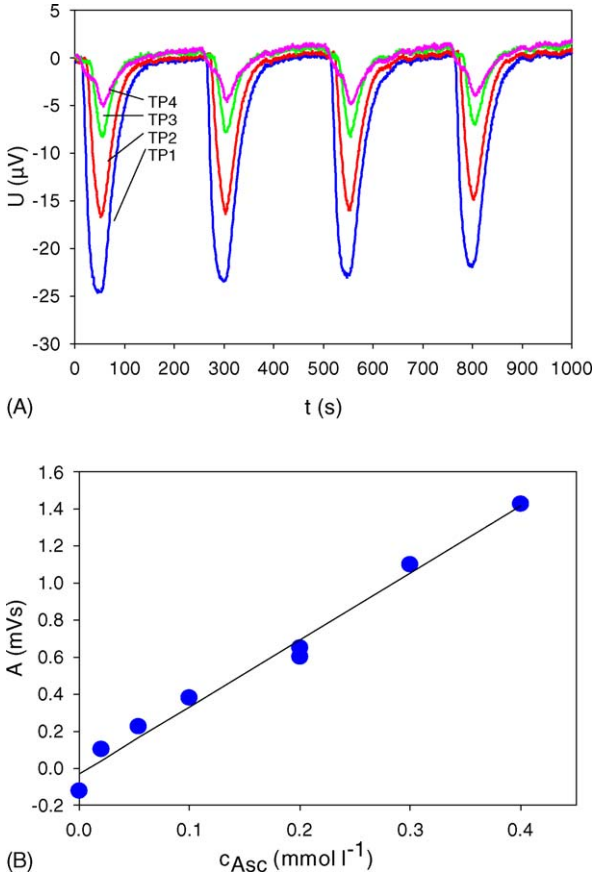

Fig. 9. Oxidation of ascorbic acid by ascorbate oxidase (A: $c = 0.4$ mmol l^{-1}).

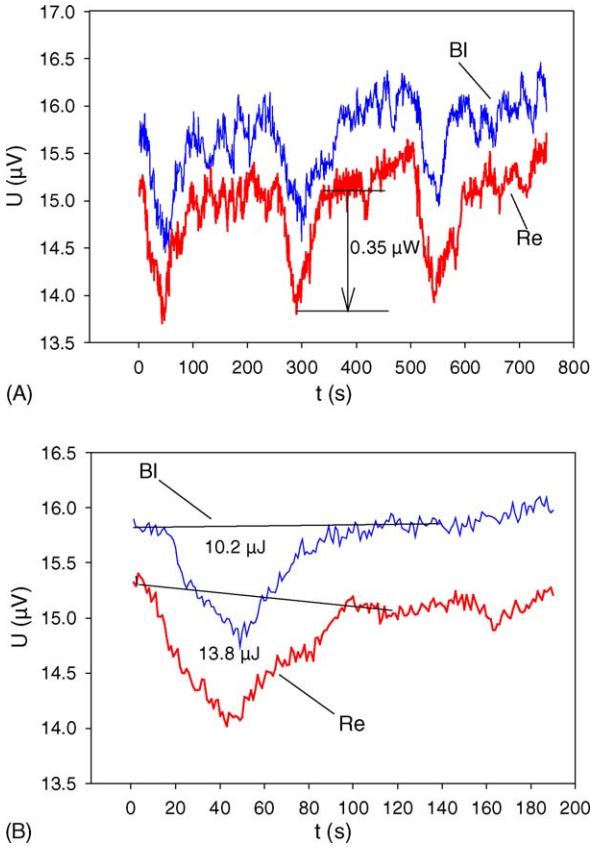

Fig. 10. Injection of 7.5 µl ascorbic acid with $c = 20$ µmol l^{-1}. (A) Signal peaks and (B) averaged peak. Bl: blank effect, Re: reaction.

pension taken from a bioreactor. The activity of *Escherichia coli* biofilms established at the membrane of the calorimetric chip. Experimental conditions and detailed results will be published in [16]. In the presented paper, we demonstrate the characterization of enzyme catalyzed reactions. Examples are explained below for illustration of the potential of the device. In the upper part of Figs. 7–9 the thermopile signals measured for a series of injected volumes are depicted. In the lower part the dependency of the cumulated signal peak area on the concentration of the substrate for each reaction is shown. The molar reaction enthalpies derived from the slopes of the curves agree with literature data: oxidation of glucose, −209 kJ mol^{-1} (−225 kJ mol^{-1} [17]); oxidation of ascorbic acid, −115 kJ mol^{-1} (−150 kJ mol^{-1} [18]); hydrolysis of penicillin G, −76 kJ mol^{-1} (−78 kJ mol^{-1} [19]). The relations of the peak heights related to the four thermopiles are different for the three reactions due to their different kinetics.

Rather high enzyme activities were chosen in order to demonstrate the concentration limits for the substrate detection. In Fig. 10 a series of signal peaks due to the injection of 7.5 µl of 20 µmol l^{-1} ascorbic acid is shown. The base line noise of 200 nV and a blank signal of 1 µV provides a noise equivalent concentration of 20 µmol l^{-1} for ascorbic acid. The related noise equivalent power is less than 50 nW. The blank experiment indicates an incomplete temperature adaptation of the injected liquid.

4. Conclusions

Design and measurements on a micro-fluid silicon chip based calorimeter have been presented. The device was optimized for the use of slow reaction at nano-watt heat power level, i.e. the sample volume of 10–20 µl is largely enough to provide a volume specific detection limit of a few mW l^{-1}. On the other hand the advantage of small substance consumption and flexible response of the calorimeter remains. Initial tests show that enzyme catalyzed reactions can be measured. The achieved volume specific detection limit and the fast response of the system permit the real-time monitoring of biochemical processes.

Acknowledgements

Financial support of German Research Council (Deutsche Forschungsgemeinschaft, Wo576/5-3) and AiF (BMWA, AiF-Nr. 13328 BR) is gratefully acknowledged.

References

[1] A.E. Beezer (Ed.), Biological Microcalorimetry, Academic Press Inc, London, 1980.

[2] Y. Zhang, S. Tadigadapa, Biosens. Bioelectr. 19 (2004) 1733–1743.

[3] E.A. Johannessen, J.M.R. Weaver, L. Bourova, P. Svoboda, P.H. Cobbold, J.M. Cooper, Anal. Chem. 74 (2002) 2190–2197.

[4] F.E. Torres, P. Kuhn, D. de Bruyker, A.G. Bell, M.V. Wolkin, E. Peeters, J.R. Williamson, G.B. Anderson, G.P. Schmitz, M.I. Recht, S. Schweizer, L.G. Scott, H.J. Ho, S.A. Elrod, P.G. Schultz, R.A. Lerner, R.H. Bruce, PNAS 101 (2004) 9517–9522.

[5] www.vivactis.de.

[6] J. Lerchner, A. Wolf, A. Weber, R. Huettl, G. Wolf, J.M. Koehler, M. Zieren, Microreaction Technology: Industrial Prospects, in: Proceedings of the International Conference on Microreaction Technology, 3rd, Frankfurt, Apr. 18–21, 1999, pp. 469–478.

[7] J. Lerchner, A. Wolf, R. Hüttl, G. Wolf, Chem. Eng. J. 101 (2004) 187–194.

[8] M. Zieren, R. Willnauer, J.M. Köhler, 4th International Symposium on Micro Total Analysis μTAS 2000, May 14–18, Enschede, Netherlands, 2000.

[9] V. Baier, R. Föhdisch, A. Ihring, E. Kessler, J. Lerchner, G. Wolf, J.M. Köhler, M. Nietzsch, M. Krügel, Sens. Actuat. B, in press.

[10] L. Ljung, Systems Identification: Theory for the User, Prentice Hall, Englewood Cliffs, NJ, 1987.

[11] J. Lerchner, G. Wolf, A. Torralba, V. Torra, Thermochim. Acta 302 (1997) 201–210.

[12] C. Auguet, J. Lerchner, V. Torra, G. Wolf, J. Therm. Anal. Cal. 71 (2003) 407–419.

[13] J. Lerchner, A. Wolf, G. Wolf, V. Torra, J. Therm. Anal. Cal., in press.

[14] H.J. Buschmann, E. Schollmeyer, Thermochim. Acta 333 (1999) 49–53.

[15] M.A.A. O'Neill, A.E. Beezer, C. Labetoulle, L. Nicolaides, J.C. Mitchell, J.A. Orchard, J.A. Connor, R.B. Kemp, D. Olomolaiye, Thermochim. Acta 399 (2003) 63–71.

[16] Th. Maskow, J. Lerchner, M. Peitzsch, H. Harms, G. Wolf, J. Biotechnol., in press.

[17] BRENDA-The Comprehensive Enzyme Information System, 2001, www.brenda.uni-koeln.de.

[18] A. Wolf, Diss. TU Bergakademie Freiberg (2003).

[19] R.N. Goldberg, Y.B. Tewari, M. Tung, Thermodynamics of Enzyme Catalyzed Reactions, NIST Standard Reference Database 74, www.bmcd.nist.gov.8080/enzyme/ename.html.